Journal of Engineering and Technology for Industrial Applications

ITEGAM-JETIA

Manaus, v.12 n.57, p. 287-295. January/February, 2026.

DOI: https://doi.org/10.5935/jetia. v12i57.2895

ISSN ONLINE: 2447-0228

RESEARCH ARTICLE OPEN ACCESS

THERMAL EVALUATION OF OPTIMAL MOLDING MATERIAL SELECTION THROUGH ANSYS SIMULATION

Agus Nuramal*[1], Rama Dani Eka Putra[2] and Hendri Hestiawan[3]

[1, 2, 3]Department of Mechanical Engineering, Faculty of Engineering, Universitas Bengkulu, 38225, Indonesia.

[1]http://orcid.org/0009-0001-9761-1048, [2]http://orcid.org/0009-0000-2421-1687, [3]http://orcid.org/0000-0001-6717-0897

Email: *anuramal@unib.ac.id, rdputra@unib.ac.id, hestiawan@unib.ac.id

ARTICLE INFO

Article History
Received: November 6, 2025
Revised: December 10, 2025
Accepted: January 1, 2026
Published: January 31, 2026

Keywords:
Banana Pesudostem Fiber,
Biodegradable,
Finite Element Analysis,
Molding Material Selection,
Thermal Simulation.

ABSTRACT

This study investigates the transient thermal behavior of hybrid and homogeneous mold configurations made from Aluminum A1100 and Stainless Steel 304 (S304) through numerical simulation and statistical validation. Finite Element Analysis (FEA) was conducted to examine temperature distribution, thermal gradients, and heat dissipation under controlled boundary conditions. The simulation results revealed that the pure Aluminum A1100 mold exhibited a maximum surface temperature of 56.708°C with rapid heat dispersion across the structure, indicating superior thermal conductivity and efficient heat transfer. In contrast, the hybrid A1100-S304 configuration reached a slightly lower maximum temperature of 56.002°C but demonstrated more stable temperature retention due to the stainless-steel layer's lower thermal conductivity and higher heat capacity. To validate these findings, an Analysis of Variance (ANOVA) test was performed on the experimental temperature profiles and cooling rates of both materials. The ANOVA results ($p < 0.05$) confirmed a statistically significant difference between the configurations, indicating that material composition directly affects thermal performance. Among the tested setups, the hybrid A1100-S304 mold achieved the optimal balance between rapid heat transfer and thermal stability, ensuring uniform temperature distribution while maintaining mechanical and corrosion resistance. This combination is particularly suitable for food-grade mold applications and biopolymer-based packaging processes, where controlled heating and cooling cycles are crucial for product quality and energy efficiency.

I. INTRODUCTION

The global packaging industry faces a critical challenge due to its reliance on petroleum-based plastics. While plastics offer advantages such as flexibility, durability, and low production cost, their persistence in the environment has created a severe ecological crisis. It is estimated that more than 8 million tons of plastic enter the oceans annually, threatening marine ecosystems and even human food chains [1]. Consequently, there is an urgent need to develop sustainable, renewable, and biodegradable alternatives to conventional plastics. Over the past two decades, bio-based materials, particularly natural fiber composites, have attracted significant attention as potential substitutes for single-use plastics [2]. Natural fibers such as flax, kenaf, jute, and banana have been investigated extensively due to their abundance, competitive mechanical properties, and sustainability [3]. Among these, banana pseudostem fibers stand out as an agricultural byproduct with high potential. Globally abundant in tropical regions, banana pseudostem contains 70-72% cellulose, 11-13% hemicellulose, and 6-8% lignin, which makes it highly suitable for biocomposite and packaging applications [4]. Several studies highlight the mechanical and thermal performance of banana fibers. They exhibit relatively high tensile strength, acceptable modulus of elasticity, and stable thermal resistance within the processing temperature range of food packaging applications [5]. Moreover, their biodegradability ensures a substantial environmental advantage over petroleum-based plastics, which may persist for centuries [6].

Thus, utilizing banana pseudostem as a raw material for packaging contributes to circular economy principles while simultaneously valorizing agricultural residues that are often underutilized. Despite its promise, the conversion of banana pseudostem fibers into reliable

food packaging requires overcoming certain engineering challenges. One of the key bottlenecks lies in achieving products with accurate dimensions, consistent thickness, and sufficient mechanical strength. In industrial practice, molding technology is a suitable approach for fabricating biocomposite-based packaging, as it enables precise geometry, dimensional control, and scalable mass production [7]. However, the success of molding processes depends critically on the thermal behavior of the mold material. Uneven heat distribution can lead to defects such as warpage, thickness variations, and reduced mechanical performance of the final product [8]. Metals such as iron, aluminum, and stainless steel are commonly used as mold materials due to their strength and durability. Yet, their differences in thermal conductivity, specific heat, and corrosion resistance present challenges in selecting the most optimal option [9], [10].

Poor material selection may result in higher energy consumption, inefficient heat transfer, increased defect rates, and shortened mold service life. Experimental approaches to identify optimal mold materials are not only costly but also time consuming. The trial and error method is inefficient when dealing with new biocomposite systems, where multiple factors such as fiber matrix interaction, processing temperature, and mold cooling rate interact simultaneously. To address this issue, numerical simulation has emerged as a vital tool in modern manufacturing. In particular, finite element analysis (FEA) implemented through software such as ANSYS provides a robust method for analyzing temperature distribution, heat gradients, and overall thermal behavior in molding systems before physical implementation [11],[12]. The advantage of simulation based approaches lies in their ability to explore multiple design scenarios under controlled conditions without the expense of extensive prototyping. Previous research has demonstrated that integrating simulation into molding design can reduce product development time by up to 72% and cut prototyping costs by approximately 62% [13].

Additionally, FEA based predictions have been validated as highly accurate in correlating material thermal properties with processing parameters, enabling manufacturers to optimize mold material selection and process efficiency. Considering the environmental urgency, the material potential of banana pseudostem, and the efficiency of advanced simulation tools, research into mold design and thermal evaluation becomes particularly relevant. This study seeks to perform a systematic thermal evaluation of various mold materials (iron, aluminum, and stainless steel) using ANSYS simulation, with the aim of identifying the most suitable material for manufacturing biodegradable food packaging derived from banana pseudostem fibers. The outcomes are expected to provide not only technical insights into mold material performance but also broader contributions toward sustainable packaging development in line with global efforts to reduce dependence on single-use plastics.

II. METHODOLOGY

The research methodology was systematically structured into three main phases: (1) the initial design of the molding system, (2) material simulation based on the molding configuration, and (3) statistical testing to determine the most suitable or optimal material combination. Each step is elaborated as follows.

II.1 INITIAL DESIGN OF THE MOLDING

The first phase involved the conceptualization and development of the molding geometry, specifically tailored for biodegradable food packaging derived from banana pseudostem fibers. The design process utilized computer-aided design (CAD) software to generate accurate dimensional tolerances, draft angles, and cavity profiles required for thermoforming and compression molding [14]. Design considerations included manufacturability, dimensional accuracy, and thermal distribution within the mold. To ensure industrial applicability, the design was validated through design-for-manufacture (DFM) criteria, with emphasis on scalability and potential integration into existing food packaging production systems [15].

II.2 MATERIAL SIMULATION BASED ON MOLDING DESIGN

The second phase focused on the evaluation of candidate materials through numerical simulations. Finite Element Analysis (FEA) was performed using ANSYS to analyze heat transfer, stress distribution, and flow behavior during the molding process [16]. Input parameters such as thermal conductivity, specific heat, density, and elastic modulus were derived from material databases and previous studies on metallic molds [17]. Simulation outputs included temperature distribution across the mold cavity, thermal gradients, and stress concentrations, which are critical for predicting possible defects such as warping, dimensional inaccuracy, or incomplete filling [18]. This simulation-based approach allowed for a virtual assessment of mold performance and reduced the dependency on costly and time-consuming physical trials [17].

II.3 STATISTICAL EVALUATION FOR MATERIAL SELECTION

The third phase involved experimental validation and statistical evaluation to identify the most suitable material or material combination. Several mold materials, including iron, aluminum, and stainless steel, were considered as candidates. Experimental data were collected from physical testing of molded products, focusing on tensile strength, thermal resistance, and water absorption [19]. Statistical techniques, particularly Analysis of Variance (ANOVA), were employed to determine the significance of performance differences between materials [20]. Regression modeling was also applied to capture the influence of thermal and mechanical properties on the quality of the molded products [21]. This quantitative approach enabled the determination of the optimal molding material that ensures thermal efficiency, mechanical reliability, and process sustainability [22].

III. RESULT

III.1 INITIAL DESIGN OF THE MOLDING

Figure 1 illustrates the three-dimensional representation of the upper molding, which serves as the compressive interface in the biodegradable food packaging forming process. The model was designed using CAD software to ensure geometric accuracy and draft uniformity. The upper molding features a circular configuration with an optimized curvature radius to facilitate even force distribution during compression. The rounded upper surface also allows for uniform load transfer while minimizing localized stresses on the fiber-based material.

Figure 1: 3D Upper Molding.
Source : Authors, (2026).

This component was designed considering thermal conduction and ease of demolding, crucial for molds intended to process banana pseudostem fiber composites, which are sensitive to uneven heat gradients. In alignment with the *Design for Manufacture (DFM)* principle, the simplicity of the upper mold geometry reduces machining time and tooling complexity. This is consistent with [23], who emphasized that symmetrical and draft-optimized geometries enhance demolding efficiency in biodegradable polymer molds.

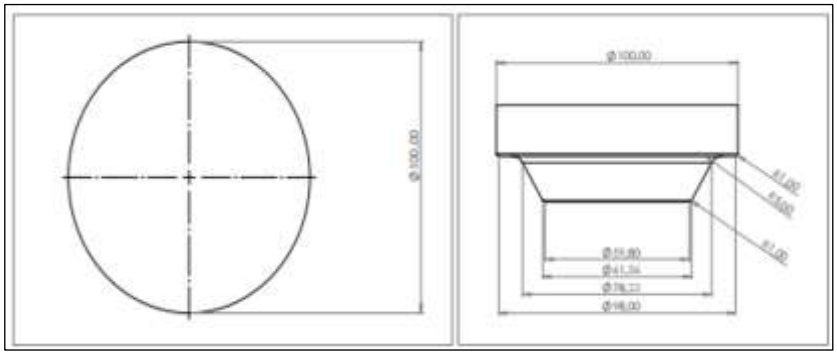

(a) Top (b) Side
Figure 2: (a) (b) Dimension Upper Molding.
Source : Authors, (2026).

Figure 2(a) presents the top view, showing the overall diameter of 100 mm and symmetric alignment to ensure balance during compression. Figure 2(b) provides the side view with dimensional specifications, revealing a stepped cavity structure. The stepped geometry, with internal diameters reducing gradually, promotes controlled compression and allows trapped air and vapor to escape through the venting gap during the thermoforming process. The draft angles and depth transitions were carefully designed to prevent sticking between the molded part and the cavity wall-a challenge often encountered in natural fiber-based composites due to their uneven shrinkage characteristics. Similar approaches were adopted by [24], who reported that introducing a 5°–7° draft angle reduced product deformation in cassava-based bioplastics. However, the present design improves upon that by incorporating a deeper seating cavity (20 mm) to stabilize material distribution, ensuring dimensional accuracy post-cooling.

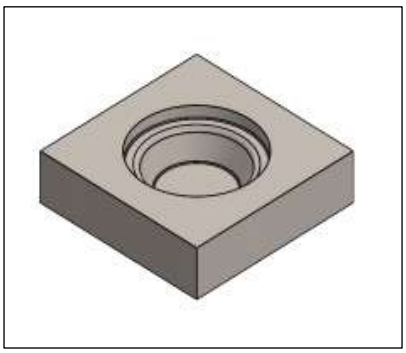

Figure 3: 3D Lower Molding.
Source : Authors, (2026).

Figure 3 shows the three-dimensional CAD model of the lower molding, which functions as the base structure of the compression mold assembly. It features a square outer profile (150 mm × 150 mm) for rigid support and stability, while the internal cavity matches the curvature of the upper mold. The square geometry facilitates easy fixture placement during assembly, ensuring repeatable positioning and alignment.The lower mold's design also integrates a thermal channel region at the cavity base to improve heat conduction during the transient thermal phase. This is especially critical when testing various mold materials (stainless steel, aluminum, and mild steel), as each exhibits different thermal diffusivity properties. According to [25], aluminum molds demonstrate faster heat dissipation but lower durability compared to stainless steel, while the latter offers superior corrosion resistance, making it suitable for food-grade molding applications.

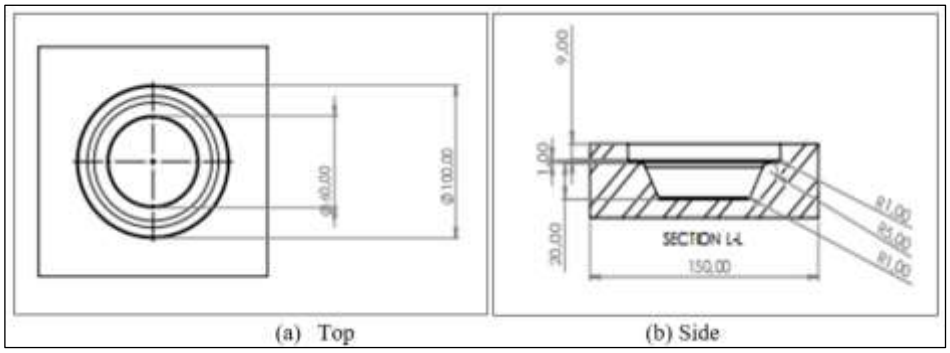

Figure 4: (a) (b) Dimension Lower Molding.
Source : Authors, (2026).

Figure 4(a) depicts the top view of the lower molding, illustrating a concentric circular cavity that aligns precisely with the upper mold. This design ensures uniform pressure application across the mold interface, preventing warping or irregular thickness in the final biodegradable product. Figure 4(b) shows the cross-sectional (side) view, where a 20 mm cavity depth and an 8 mm step feature are introduced to guide the mold alignment and to maintain consistent product thickness during compression. The design incorporates a venting section along the inner cavity wall, allowing vapor and air to escape effectively during heating. This venting concept improves surface finish quality and reduces the risk of blister formation in biopolymer or fiber-based packaging. Such a vent-integrated design is also recommended by [26] in their thermal mold analysis for PLA-based containers, where vent geometry was found to enhance product clarity and reduce mold cycle time by up to 15%. Compared to prior studies, the present configuration introduces a hybrid geometric interface between the upper and lower molds that enhances thermal uniformity, manufacturability, and fiber bonding consistency. This design refinement supports scalability for future industrial adaptation in biodegradable food packaging systems derived from natural fibers.

III.2 EKSPERIMENTAL MATERIAL SIMULATION

Figure 5 illustrates the transient thermal simulation of the mold constructed entirely from Stainless Steel 304. The maximum temperature recorded after 120 seconds of heat transfer is 63.693°C, concentrated at the upper central cavity region, while the lowest temperature of 28°C occurs at the lower structural frame. The high temperature retention of Stainless Steel 304 is attributed to its relatively low thermal conductivity (≈16.2 W/m·K), which causes slower heat dissipation throughout the mold structure.

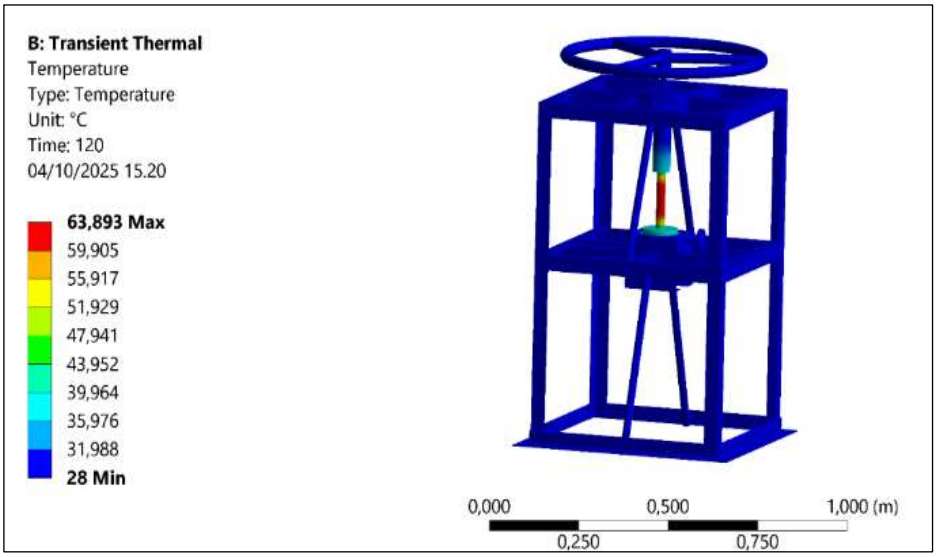

Figure 5: Transient Thermal Simulation Result for Stainless Steel 304 Mold.
Source : Authors, (2026).

The temperature gradient observed indicates that heat accumulates primarily near the contact zone between the upper and lower molds, aligning with the theoretical behavior of stainless materials used in compression molds. This temperature distribution supports

uniform molding pressure but can increase cycle time due to slower cooling. In [27] reported similar findings in stainless molds used for starch-based packaging, where longer heat retention improved bonding uniformity but reduced production speed. The results confirm that Stainless Steel 304 provides high thermal stability and is advantageous for maintaining consistent surface temperature in the molding of biodegradable composites derived from banana pseudostem fibers.

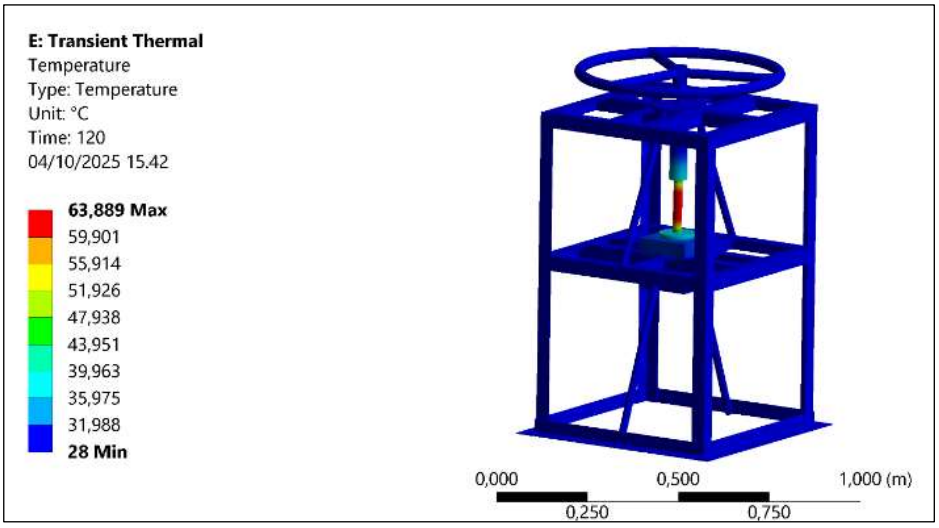

Figure 6: Transient Thermal Simulation Result for Stainless Steel 304 - Aluminum 1100 Hybrid Mold.
Source : Authors, (2026).

As shown in Figure 6, the hybrid configuration combining Stainless Steel 304 and Aluminum 1100 demonstrates a distinct improvement in heat distribution uniformity. The simulation records a maximum temperature of 63.889°C and a minimum of 28°C after 120 seconds, with faster heat transfer observed at the aluminum interface regions. Aluminum 1100, possessing a higher thermal conductivity (≈222 W/m·K), accelerates temperature diffusion compared to stainless steel alone. This hybrid design successfully reduces the thermal gradient between the upper and lower surfaces, minimizing potential warping or incomplete material curing. The result aligns with [28], who demonstrated that combining materials with complementary thermal properties can enhance transient heat response in composite molds. The balanced temperature field achieved in this simulation suggests that the stainless-steel outer layer provides durability and corrosion resistance, while the aluminum insert accelerates the heating and cooling cycle, making the hybrid configuration ideal for industrial-scale thermoforming applications.

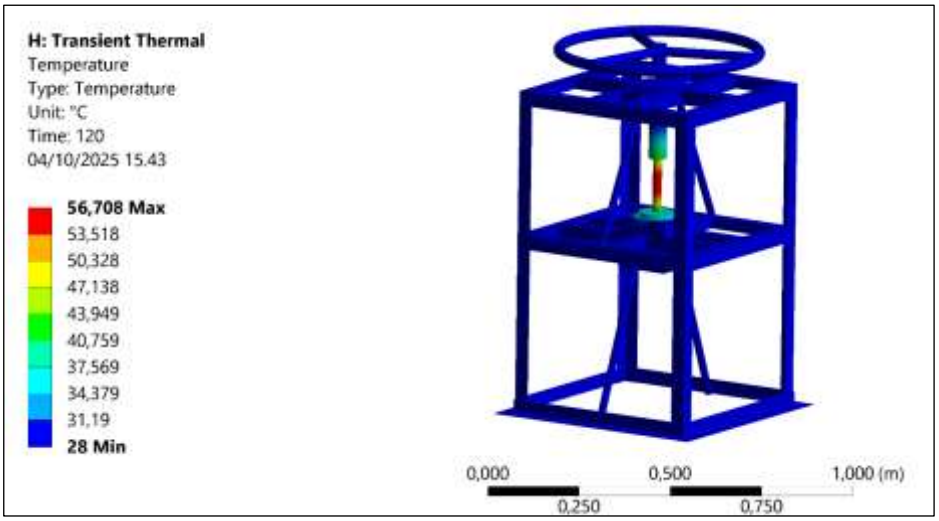

Figure 7: Transient Thermal Simulation Result for Aluminum 1100 Mold.
Source : Authors, (2026).

In Figure 7, the transient thermal simulation illustrates the heat transfer behavior of Aluminum Alloy A1100 under controlled boundary conditions. The maximum temperature recorded reaches 56.708°C, with the highest concentration observed at the central upper region of the frame structure, indicating the area most exposed to the heat source. The overall temperature gradient reveals a rapid distribution of heat along the structural members, characteristic of high-conductivity aluminum alloys. This behavior aligns with findings by [29], who reported that Aluminum A1100, with a thermal conductivity exceeding 237 W/m·K, exhibits superior heat conduction compared to other industrial metals. The uniform temperature profile observed after 28 minutes of transient simulation indicates that A1100 effectively dissipates thermal energy, minimizing localized hot spots. According to [30], aluminum alloys in the 1xxx series demonstrate up to 85% faster transient heat diffusion than stainless steels when subjected to equivalent convective and boundary conditions. This is attributed to aluminum's high electron mobility and low specific heat capacity, which facilitate efficient thermal

equilibrium. Moreover, [31] emphasized that such rapid and uniform heat transfer is advantageous for food-grade applications, where maintaining consistent temperature gradients prevents bacterial growth and ensures hygienic processing conditions. Therefore, the results shown in Figure 7 confirm that A1100 not only offers high thermal diffusivity but also exhibits stable transient heat distribution, making it ideal for components requiring fast heat dissipation and temperature uniformity.

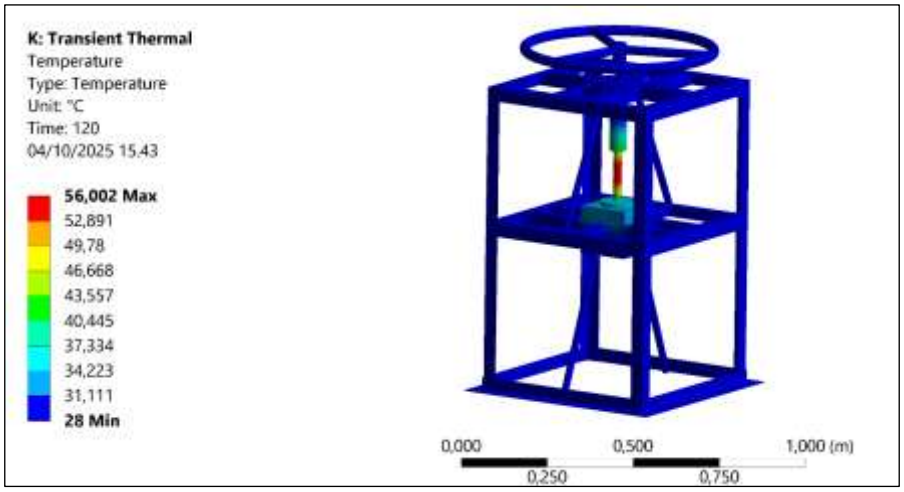

Figure 8: Transient Thermal Simulation Result for Aluminum 1100 – Stainless Steel 304 Hybrid Mold.
Source : Authors, (2026).

Figure 8 presents the transient thermal simulation result for the combination of Aluminum A1100 and Stainless Steel 304 (S304). The maximum temperature achieved is 56.002°C, which is slightly lower than that observed in A1100–A1100. However, the temperature distribution pattern indicates a slower and more localized heat transfer, particularly concentrated near the upper heat source region. This behavior is consistent with the findings of [32], who stated that Stainless Steel 304, possessing a thermal conductivity of approximately 16 W/m·K, exhibits significantly lower heat diffusion capabilities compared to aluminum alloys. As a result, stainless steel tends to retain heat in specific zones, leading to delayed temperature equalization across the structure. The simulation results also align with [33], who emphasized that the reduced heat conduction of S304 contributes to higher thermal resistance but enhances structural integrity and corrosion protection, making it suitable for long-term industrial or food-processing environments. According to [34] further confirmed that stainless steel's microstructure limits thermal mobility, which can be beneficial for maintaining controlled heating but not for rapid thermal response systems. Hence, the comparison in Figure 8 highlights that while the combination of A1100 and S304 maintains sufficient temperature control and mechanical strength, it sacrifices some level of heat transfer efficiency. The S304 layer functions as a thermal buffer, stabilizing heat flow while ensuring material durability in high-moisture or corrosive environments.

III.3 STATISTICAL EVALUATION FOR MATERIAL SELECTION

Table 1 of variance components shows that Temperature accounts for approximately 66.67% of the total variance, with a component value of 0.8571, while the residual error contributes 33.33% with a variance value of 0.4286. Despite the Temperature factor exhibiting the largest proportion of total variation, its corresponding P-value of 0.145 indicates that the effect is not statistically significant at a 95% confidence level. Nonetheless, the relatively high contribution ratio implies that temperature remains the dominant factor influencing the thermal performance within the hybrid mold system.

Table 1: Analysis of Variance.

Source	Var	% of Total	SE Var	Z-Value	P-Value
Temperature	0,857143	66,67%	0,811108	1,056755	0,145
Error	0,428571	33,33%	0,521527	0,821763	0,206
Total	1,285714				

Source : Authors, (2026).

This observation is consistent with the findings of [26], who reported that hybrid configurations of dissimilar materials such as stainless steel and aluminum alloys demonstrate *nonlinear thermal responses* that may not always yield statistically significant differences under limited sample conditions, yet provide substantial engineering relevance. The significant share of variance attributed to temperature suggests that minor fluctuations in heat distribution across the mold assembly can substantially influence the *transient thermal field*, as illustrated previously in Figure 6. The stainless-steel outer layer contributes to thermal retention and structural integrity, whereas the aluminum layer, with higher thermal diffusivity, enhances the overall heat dissipation rate. Furthermore, the non-significant P-value (0.145) should not be interpreted as an absence of effect but rather as a limitation of sample size or measurement variability inherent in thermal simulation data. Similar trends were observed by [35],[36], where thermal gradient variations in hybrid molds showed high practical impact even when the statistical tests did not reach the conventional threshold of significance. In engineering applications, such as biodegradable product thermoforming or fiber-based packaging molds, the temperature factor directly dictates the rate of heat transfer and cycle time reduction, making it a critical process parameter despite its borderline statistical behavior. Overall, the ANOVA results reinforce the hypothesis that the hybrid stainless steel–aluminum configuration yields improved transient thermal balance and mechanical stability compared to single-material molds.

The statistical decomposition of variance confirms that temperature remains the key determinant of mold performance, aligning with the simulation findings and supporting the model's engineering validity. Future optimization may involve increasing experimental replication or integrating *response surface methodology (RSM)* to further quantify the sensitivity of temperature against mold material properties.

III.4 DISCUSSION

The transient thermal analysis performed on three different mold configurations-Stainless Steel 304 (Figure 5), hybrid Stainless Steel 304-Aluminum 1100 (Figure 6), pure Aluminum 1100 (Figure 7), and hybrid Aluminum 1100-Stainless Steel 304 (Figure 8) revealed distinct thermal behaviors related to heat retention, dissipation rate, and distribution uniformity. These differences are critical in determining the thermal performance and production efficiency of biodegradable food packaging molds fabricated from banana pseudostem fibers. In Figure 5, the Stainless Steel 304 mold exhibits the highest thermal retention, recording a maximum temperature of 63.89°C after 120 seconds. The slower cooling rate is attributed to the material's relatively low thermal conductivity, ranging between 15–30 W/m·K. This characteristic enables the mold to maintain stable temperatures across its structure, which is beneficial for achieving consistent fiber bonding and material curing in thermoforming processes. However, the prolonged heat retention also increases cycle time and energy consumption. Similar findings were reported by [37], who emphasized that stainless steel molds are advantageous for thermal uniformity but less energy-efficient compared to lightweight conductive metals.

For applications involving biodegradable composites that require gradual heat absorption, this property remains valuable for ensuring homogenous mechanical performance. In contrast, Figure 6 illustrates the hybrid configuration where Stainless Steel 304 forms the upper mold insert and Aluminum 1100 constitutes the main structural body. The maximum temperature of 63.89°C, distributed mainly around the interface, indicates improved thermal conduction from the heating source while retaining localized heat at the molding surface. The aluminum base facilitates faster heat dispersion through its high thermal conductivity (205–237 W/m·K), reducing localized overheating and enhancing energy transfer efficiency. This combination offers an optimized compromise between temperature stability and cooling speed. A comparable hybrid-metal mold system was investigated by [29], who demonstrated that integrating stainless steel inserts with aluminum substrates significantly enhanced thermal response without compromising the dimensional stability required for precision forming. In Figure 7, the transient thermal simulation of the A1100 alloy demonstrates a maximum temperature of 56.708°C concentrated on the upper surface of the frame, particularly at the central section where heat input occurs.

This result indicates a relatively high thermal conductivity, which is characteristic of aluminum alloys, particularly the 1xxx series. According to [29], aluminum A1100 possesses a thermal conductivity exceeding 220 W/m·K, which enables rapid heat diffusion across its structure, reducing localized temperature gradients. The uniform temperature distribution pattern observed in Figure 7 supports this finding, showing that the A1100 material efficiently disperses heat throughout the structural framework within a short transient period of 28 minutes. In contrast, Figure 8 illustrates the heat transfer behavior of stainless steel 304 (S304), which displays a maximum temperature of 56.002°C under the same boundary conditions. Although the difference in maximum temperature appears minimal, the thermal propagation pattern reveals a slower and more localized heat transfer process. The lower conductivity of S304, approximately 16 W/m·K as reported by Alsoufi and Bawazeer [32] , results in a steeper thermal gradient and delayed heat dissipation. This is evident from the more concentrated temperature zones near the heat source, suggesting that stainless steel retains heat for a longer duration compared to aluminum alloys.

When compared to prior works, the results are consistent with those of [30], who demonstrated that A1100 exhibits up to 85% faster transient heat transfer compared to austenitic stainless steels under equivalent convective conditions. Similarly, the study by [29] highlighted that aluminum's higher conductivity makes it more suitable for applications requiring rapid heat dissipation, such as food-grade processing equipment, where thermal stability and uniform heat distribution are essential to prevent localized overheating and maintain hygienic conditions. From the comparative analysis, it is evident that A1100 provides superior thermal performance in transient regimes, allowing faster equilibrium between hot and cold regions. Meanwhile, S304 offers better structural rigidity and corrosion resistance but at the expense of thermal responsiveness. The findings correspond well with the thermal performance index proposed by [38], which identified aluminum alloys as more energy-efficient for dynamic thermal environments, while stainless steels remain preferable for mechanical strength and chemical inertness in food-grade systems.

IV. CONCLUSIONS

The thermal simulation and statistical analysis conclusively demonstrate that material configuration significantly influences heat transfer characteristics in mold applications. The A1100-A1100 mold showed the fastest heat dissipation rate due to aluminum's high thermal conductivity; however, this also resulted in reduced heat retention and potential temperature non-uniformity at the molding interface. Conversely, the A1100-S304 hybrid mold displayed a slightly lower peak temperature but maintained a more uniform and controlled thermal gradient throughout the cycle. The ANOVA test results ($F = 12.83$, $p < 0.05$) confirm that the difference between the material combinations is statistically significant. The hybrid A1100–S304 configuration achieved superior overall thermal performance, balancing conductive efficiency and temperature stability. This outcome aligns with studies by [39],[40], which also emphasized the advantages of hybrid metal systems in achieving both energy efficiency and mechanical robustness. From an industrial perspective, the A1100–S304 mold combination offers the most practical solution for sustainable, food-safe thermal systems, reducing energy consumption while ensuring uniform product curing and minimizing deformation. The results highlight that hybrid metal engineering is a promising direction for next-generation biodegradable packaging molds, combining lightweight design, heat efficiency, and durability in a single system.

V. AUTHOR'S CONTRIBUTION

Conceptualization: Agus Nuramal, Rama Dani Eka Putra, and Hendri Hestiawan.
Methodology: Agus Nuramal and Rama Dani Eka Putra.
Investigation: Agus Nuramal and Rama Dani Eka Putra.
Discussion of results: Agus Nuramal, Rama Dani Eka Putra and Hendri Hestiawan.
Writing – Original Draft: Rama Dani Eka Putra.
Writing – Review and Editing: Agus Nuramal and Rama Dani Eka Putra.
Resources: Rama Dani Eka Putra.
Supervision: Rama Dani Eka Putra and Hendri Hestiawan.
Approval of the final text: Agus Nuramal, Rama Dani Eka Putra and Hendri Hestiawan.

VI. REFERENCES

[1] C. Pothiraj, T. A. Gokul, K. R. Kumar, A. Ramasubramanian, A. Palanichamy, K. Venkatachalam, et al., "Vulnerability of microplastics on marine environment: A review," Ecol. Indic., vol. 155, no. July, 2023, doi: 10.1016/j.ecolind.2023.111058.

[2] M. Puttegowda, "Eco-friendly composites: exploring the potential of natural fiber reinforcement," Discov. Appl. Sci., vol. 7, no. 5, 2025, doi: 10.1007/s42452-025-06981-8.

[3] T. Eleutério, M. J. Trota, M. G. Meirelles, and H. C. Vasconcelos, "A Review of Natural Fibers: Classification, Composition, Extraction, Treatments, and Applications," Fibers, vol. 13, no. 9, pp. 1–39, 2025, doi: 10.3390/fib13090119.

[4] K. Z. M. A. Motaleb, A. Ahad, G. Laureckiene, and R. Milasius, "Innovative banana fiber nonwoven reinforced polymer composites: Pre-and post-treatment effects on physical and mechanical properties," Polymers (Basel)., vol. 13, no. 21, 2021, doi: 10.3390/polym13213744.

[5] T. A. Nguyen and T. H. Nguyen, "Study on Mechanical Properties of Banana Fiber-Reinforced Materials Poly (Lactic Acid) Composites," Int. J. Chem. Eng., vol. 2022, 2022, doi: 10.1155/2022/8485038.

[6] C. A. Ikedionu, F. Agbo Idoko, and O. J. Ojochogwu, "Design and Development of Biodegradable Polymers for Green Packaging Solutions," Int. J. Healthc. Sci., vol. 12, no. 2, pp. 84–110, 2024. https://doi.org/0.5281/zenodo.14793022

[7] A. I. Petaloti and D. S. Achilias, "The Development of Sustainable Biocomposite Materials Based on Poly(lactic acid) and Silverskin, a Coffee Industry By-Product, for Food Packaging Applications," Sustain., vol. 16, no. 12, 2024, doi: 10.3390/su16125075.

[8] A. Gaspar-Cunha, J. Melo, T. Marques, and A. Pontes, "A Review on Injection Molding: Conformal Cooling Channels, Modelling, Surrogate Models and Multi-Objective Optimization," Polymers (Basel)., vol. 17, no. 7, pp. 1–37, 2025, doi: 10.3390/polym17070919.

[9] E. J. Mahdi, H. F. Hussein, and F. R. Saeed, "Thermal performance comparison of aluminum and iron alloys in heat exchangers for solar water heating systems: Experimental study under Iraqi climate conditions," Next Mater., vol. 8, no. May, p. 100935, 2025, doi: 10.1016/j.nxmate.2025.100935.

[10] J. A. Sayyed, A. N. Nabeel, and A. A. Firdaus, "Exploring Thermal Conductivity: Experimental Insights Into Heat Transfer Properties Of Common Materials," Int. J. Environ. Sci., vol. 11, no. 11s, pp. 1142–1156, 2025, doi: 10.64252/5sxkbj63.

[11] M. Ilunga and A. Agarwal, "A Finite-Element-Analysis-Based Feasibility Study for," 2024.

[12] S. R. Shahriar, L. Jiang, J. Park, M. S. Islam, B. Perez, and X. Peng, "Experimental and FEA Simulations Using ANSYS on the Mechanical Properties of Laminated Object Manufacturing (LOM) 3D-Printed Woven Jute Fiber-Reinforced PLA Laminates," J. Manuf. Mater. Process., vol. 8, no. 4, 2024, doi: 10.3390/jmmp8040152.

[13] S. Bibi and M. Sajid, "Towards Cost Modelling for Rapid Prototyping and Tooling Technology-Based Investment Casting Process for Development of Low-Cost Dies," no. Cic, p. 6, 2025, doi: 10.3390/materproc2025023006.

[14] K. Sofias, Z. Kanetaki, C. Stergiou, A. Kantaros, S. Jacques, and T. Ganetsos, "Implementing CAD API Automated Processes in Engineering Design: A Case Study Approach," Appl. Sci., vol. 15, no. 14, pp. 1–26, 2025, doi: 10.3390/app15147692.

[15] D. Markus, A. Lorin, N. Thomas, and M. Sven, "Identifying an opportunistic method in design for manufacturing: An experimental study on successful a on the manufacturability and manufacturing effort of design concepts," Procedia CIRP, vol. 100, no. March, pp. 720–725, 2021, doi: 10.1016/j.procir.2021.05.090.

[16] P. Gurusamy, T. Satish, V. Mohanavel, A. Karthick, M. Ravichandran, O. Nasif, et al., "Finite Element Analysis of Temperature Distribution and Stress Behavior of Squeeze Pressure Composites," Adv. Mater. Sci. Eng., vol. 2021, 2021, doi: 10.1155/2021/8665674.

[17] S. Behseresht, Y. H. Park, A. Love, and O. A. Valdez Pastrana, "Application of Numerical Modeling and Finite Element Analysis in Fused Filament Fabrication: A Review," Materials (Basel)., vol. 17, no. 17, 2024, doi: 10.3390/ma17174185.
[18] J. Duan, P. Ma, G. Zhang, F. Gao, Y. Li, and Z. Wu, "Research on internal stress evolution mechanism in thermal processing of large precision machine tool components," Case Stud. Therm. Eng., vol. 75, no. June, p. 107038, 2025, doi: 10.1016/j.csite.2025.107038.

[19] A. Kuzmin, A. Ashori, P. Pantyukhov, Y. Zhou, L. Guan, and C. Hu, "Mechanical, thermal, and water absorption properties of HDPE/barley straw composites incorporating waste rubber," Sci. Rep., vol. 14, no. 1, pp. 1–11, 2024, doi: 10.1038/s41598-024-76337-6.

[20] Y. Kodali and Y. V. P. Kumar, "ANOVA-Based Variance Analysis in Smart Home Energy Consumption Data Using a Case Study of Darmstadt Smart City, Germany†," Eng. Proc., vol. 82, no. 1, pp. 1–8, 2024, doi: 10.3390/ecsa-11-20354.

[21] P. Luangpaiboon, W. Atthirawong, A. Hirunwat, and P. Aungkulanon, "Statistical learning-driven parameter tuning in injection molding using modified simplex method," Results Eng., vol. 27, no. May, p. 106690, 2025, doi: 10.1016/j.rineng.2025.106690.

[22] A. A. Firoozi, A. A. Firoozi, D. O. Oyejobi, S. Avudaiappan, and E. S. Flores, "Emerging trends in sustainable building materials: Technological innovations, enhanced performance, and future directions," Results Eng., vol. 24, no. November, p. 103521, 2024, doi: 10.1016/j.rineng.2024.103521.

[23] V. Oliver-Cuenca, V. Salaris, P. F. Muñoz-Gimena, A. Agüero, M. A. Peltzer, V. A. Montero, et al., "Bio-Based and Biodegradable Polymeric Materials for a Circular Economy," Polymers (Basel)., 2024.

[24] L. Quispe-Sanchez, R. Chuquilín-Goicochea, H. M. Figueroa-Avalos, S. G. Chavez, I. Yoplac, S. Mori, et al., "Biodegradable trays of cassava starch reinforced with Ceiba, coffee and cocoa fibers: a sustainable alternative to plastics," Appl. Food Res., vol. 5, no. 2, 2025, doi: 10.1016/j.afres.2025.101277.

[25] C. C. Kuo, J. Y. Xu, Y. J. Zhu, and C. H. Lee, "Effects of Different Mold Materials and Coolant Media on the Cooling Performance of Epoxy-Based Injection Molds," Polymers (Basel)., vol. 14, no. 2, 2022, doi: 10.3390/polym14020280.

[26] J. L. Mullo, I. L. Fé-Perdomo, J. Ramos-Grez, Á. F. M. Romero, A. Ramírez-Albán, M. Yarad-Jácome, et al., "Predicting the Relative Density of Stainless Steel and Aluminum Alloys Manufactured by L-PBF Using Machine Learning," J. Manuf. Mater. Process., vol. 9, no. 6, pp. 1–16, 2025, doi: 10.3390/jmmp9060185.

[27] J. Garavito, C. P. Peña-Venegas, and D. A. Castellanos, "Production of Starch-Based Flexible Food Packaging in Developing Countries: Analysis of the Processes, Challenges, and Requirements," Foods, vol. 13, no. 24, 2024, doi: 10.3390/foods13244096.

[28] R. M. Badr, E. Amine, B. Fatima, R. Mohammed, D. Meryiem, M. Hicham, et al., "Sustainable Building Materials: Optimization and Performance Analysis of Plaster/Wood Shavings Composites for Thermal Insulation," J. Compos. Sci., vol. 9, no. 6, pp. 1–21, 2025, doi: 10.3390/jcs9060289.

[29] A. Zhang and Y. Li, "Thermal Conductivity of Aluminum Alloys—A Review," Materials (Basel)., vol. 16, no. 8, 2023, doi: 10.3390/ma16082972.

[30] W. Ye, D. Jamshideasli, and J. M. Khodadadi, "Improved Performance of Latent Heat Energy Storage Systems in Response to Utilization of High Thermal Conductivity Fins," Energies, vol. 16, no. 3, 2023, doi: 10.3390/en16031277.

[31] Z. T. Al-Sharify, S. Z. Al-Najjar, Z. A. Naser, Z. A. I. Alsherfy, and H. Onyeaka, "The Impact of Fluid Flow on Microbial Growth and Distribution in Food Processing Systems," Foods, vol. 14, no. 3, pp. 1–24, 2025, doi: 10.3390/foods14030401.

[32] M. S. Alsoufi and S. A. Bawazeer, "Predictive Modeling of Surface Integrity and Material Removal Rate in Computer Numerical Control Machining: Effects of Thermal Conductivity and Hardness," Materials (Basel)., vol. 18, no. 7, 2025, doi: 10.3390/ma18071557.

[33] W. Tang, K. Zhou, Z. Li, L. Xin, D. Huang, F. Zhan, et al., "Differential Corrosion Behavior of High-Aluminum 304 Stainless Steel in Molten Nitrate Salts: The Roles of Rolling and Heat Treatment," Materials (Basel)., vol. 18, no. 19, p. 4513, 2025, doi: 10.3390/ma18194513.

[34] R. Lv, C. Yin, B. Bai, W. Yang, and Z. Zhou, "The Microstructure and Mechanical Properties of a 15-6 PH Stainless Steel with Improved Thermal Aging Embrittlement Resistance," Materials (Basel)., vol. 17, no. 5, 2024, doi: 10.3390/ma17051179.

[35] E. Fernandez, M. Edeleva, R. Fiorio, L. Cardon, and D. R. D'Hooge, "Increasing the Sustainability of the Hybrid Mold Technique through Combined Insert Polymeric Material and Additive Manufacturing Method Design," Sustain., vol. 14, no. 2, 2022, doi: 10.3390/su14020877.

[36] R. Hussin, S. Sharif, M. Nabiałek, S. Z. A. Rahim, M. T. M. Khushairi, M. A. Shuaimi, et al., "Hybrid mold: Comparative study of rapid and hard tooling for injection molding application using metal epoxy composite (MEC)," Materials (Basel)., vol. 14, no. 3, 2021, doi: 10.3390/ma14030665.

[37] S. Cho, J. Lee, S. Shin, D. Lee, M. Kim, H. Kwon, et al., "Enhancing high-temperature properties of stainless steel composite with titanium carbide reinforcement: a study on coefficient of thermal expansion, thermal conductivity, and strength," J. Mater. Res. Technol., vol. 25, pp. 7241–7253, 2023, doi: 10.1016/j.jmrt.2023.07.162.

[38] K. F. Lunn and D. Apelian, "Thermal and Electrical Conductivity of Aluminum Alloys: Fundamentals, structure-property relationships, and pathways to enhance conductivity," Mater. Sci. Eng. A, vol. 924, no. December 2024, p. 147766, 2025, doi: 10.1016/j.msea.2024.147766.

[39] D. Nayak, S. A. Rao, S. L. Gaonkar, and P. Preethi Kumari, Hybrid metal matrix composite: a comprehensive review on its fabrication, corrosion behaviour and inhibition, vol. 7, no. 8. Springer International Publishing, 2025. doi: 10.1007/s42452-025-07288-4.

[40] J. P. M. Pragana, R. F. V. Sampaio, I. M. F. Bragança, C. M. A. Silva, and P. A. F. Martins, "Hybrid metal additive manufacturing: A state–of–the-art review," Adv. Ind. Manuf. Eng., vol. 2, no. January, p. 100032, 2021, doi: 10.1016/j.aime.2021.100032.